

MODELING OF HETEROGENEOUS MATERIALS USING A MESOSCOPIC SCALE FINITE ELEMENT ANALYSIS

JOSÉ J. C. PITUBA^{*}, GABRIELA R. FERNANDES^{*} AND EDUARDO A. DE SOUZA
NETO[†]

^{*} Federal University of Goiás
Campus Catalão, Department of Civil Engineering
Campus Catalão, Av Dr Lamartine Pinto de Avelar, 1120, Catalão, 75740-020, Goiás, Brazil
email: julio.pituba@pq.cnpq.br, gabriela.fernandes@pq.cnpq.br

[†] Swansea University, Civil and Computational Engineering Centre
School of Engineering
, Singleton Park, Swansea SA2 8PP, United Kingdom
email: E.deSouzaNeto@swansea.ac.uk

Key Words: *Multi-scale Models, Ductile Porous Media, Cohesive Fracture.*

Abstract. This work presents a two-dimensional meso-scale model that captures some features of the mechanical behavior of heterogeneous material. First, it intends to describe the behavior of a metallic material using Von Mises elasto-plastic model with linear strain hardening. In rupture stages, some microcracks are created. Therefore, it is adopted a modified cohesive fracture model in order to simulate the cracking process until complete failure. The Representative Volume Element consists of elastic inclusions or cavities idealized as circular shapes placed into the metallic matrix in order to investigate the behavior of the RVEs. All simulations have been performed by employing the computational homogenization under the plane stress assumption in small strain regime. The average stress is obtained by imposing the macro-strain over the RVE and subsequently solving the microscopic initial boundary value problem for the defined boundary condition assumed. In summary, the proposed homogenization-based model is found to be a suitable tool for the identification of macroscopic constitutive response of this kind of material.

1 INTRODUCTION

Despite of the materials used in Engineering (metals, polymers, composites, concretes and woods) have different microstructures, at the macroscopic level similar characteristics of mechanical behavior are observed, as example: elasticity, viscosity, plastic strain, brittle rupture, ductile rupture, etc. Because of these similarities, constitutive models based on continuum mechanics and thermodynamics of solids applied to macroscopic analyses are usually proposed. However, it is important to note that the deformation and rupture processes take place at micro-scale level. In this context, a finite element procedure within a purely kinematical multi-scale framework proposed by [1] is used to simulate the mechanical

behaviour of ductile porous materials as well as reinforced Metal Matrix Composites (MMCs). The application of these materials is nowadays increasing due to their improved properties such as: high stiffness, low density and high tensile strength. On the other hand, these useful properties lead to poor ductility and fracture properties [2].

In the paper, a finite element procedure within a purely kinematical multi-scale framework has been used. For this purpose, a set of Representative Volume Elements (RVEs) is analyzed for initial stages of loading, when an elasto-plastic behavior is adopted and then, for rupture stages, when take place a phase debonding, an interface crack closure/opening and a cracking process in the matrix. Therefore, a modified cohesive fracture model to deal with ductile media is proposed to simulate the cracking process up to the failure. This model considers normal and tangential separation of the cohesive zone. Moreover, a Von Mises elasto-plastic model with linear strain hardening [3] is used to model the matrix behavior.

This work presents the kinematical multi-scale framework in section 2. Then, the modified cohesive fracture model is briefly presented in section 3. After that, some numerical results related to the dissipative process in the RVE are shown in section 4. Finally, in section 5 some concluding remarks are presented.

2 MULTI-SCALE CONSTITUTIVE MODELING

Let us initially consider the macro-continuum depicted in Figure 1. For the RVE the volume is denoted by V_μ , the domain by Ω_μ , the boundary by $\partial\Omega_\mu$. In order to perform the multi-scale analysis, one RVE must be associated with each point x of the macro-continuum where the stress vector computation is required. Besides, to solve the multi-scale problem one has to define the dimensions, discretisation and material properties for only one RVE, as these characteristics are the same for all RVEs defined in the macro-continuum. Note that in the case of having different materials in the macro-continuum, different RVEs should be defined.

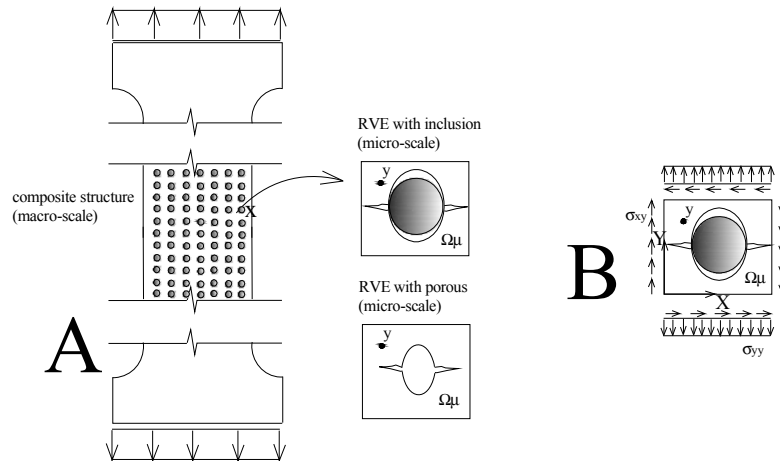


Figure 1(a) Macroscopic continuum and RVEs. (b) RVE under plane stress.

The domain of the RVE is assumed to consist in general of a solid part, Ω_μ^s , and a void part Ω_μ^v , being $\Omega_\mu = \Omega_\mu^v \cup \Omega_\mu^s$. The void part Ω_μ^v may consist of cracks and pores or may be

filled with a pressurised fluid. Note that the solid part of the RVE can be made of distinct materials (or phases), each one defined by a sub-domain, whose material can have different properties and be governed by different non-linear constitutive models.

At any instant t , the strain and stress tensors at an arbitrary point x of the macro-continuum are assumed to be the volume average of their respective microscopic field ($\boldsymbol{\varepsilon}_\mu$ or $\boldsymbol{\sigma}_\mu$), defined over the RVE domain Ω_μ :

$$\boldsymbol{\varepsilon}(x, t) = \frac{1}{V_\mu} \int_{\Omega_\mu} \boldsymbol{\varepsilon}_\mu(y, t) dV, \quad (1)$$

$$\boldsymbol{\sigma}(x, t) = \frac{1}{V_\mu} \int_{\Omega_\mu} \boldsymbol{\sigma}_\mu(y, t) dV, \quad (2)$$

where $\boldsymbol{\varepsilon}_\mu(y, t) = \nabla^s \mathbf{u}_\mu(y, t)$ is the symmetric gradient of the microscopic displacement field \mathbf{u}_μ of the RVE, while the microscopic stress $\boldsymbol{\sigma}_\mu = \boldsymbol{\sigma}_\mu(y, t)$ can be written in terms of the microscopic strain, i. e., $\boldsymbol{\sigma}_\mu(y, t) = \mathbf{f}_y(\boldsymbol{\varepsilon}_\mu(y, t))$. In this work, for the triangular elements defined in the matrix, the constitutive functional \mathbf{f}_y is defined by the Von Mises elasto-plastic criterion while for the rectangular elements defined on the interface between matrix and inclusions, the stress are computed taking into account the fracture and contact phenomena.

In general way, by the homogenization process we can also obtain the homogenised constitutive tangent modulus \mathbf{C}^{ep} , as follows:

$$\mathbf{C}^{ep}(x, t) = \frac{\partial \boldsymbol{\sigma}(x, t)}{\partial \boldsymbol{\varepsilon}(x, t)} = \frac{1}{V_\mu} \int_{\Omega_\mu} \frac{\partial \boldsymbol{\sigma}_\mu(y, t)}{\partial \boldsymbol{\varepsilon}_\mu(y, t)} dV = \frac{1}{V_\mu} \int_{\Omega_\mu} \frac{\partial \mathbf{f}_y(\boldsymbol{\varepsilon}_\mu(y, t))}{\partial \boldsymbol{\varepsilon}_\mu(y, t)} dV \quad (3)$$

Observe that after solving the RVE equilibrium problem (for more details see [4]), the microscopic fields of strain $\boldsymbol{\varepsilon}_\mu$ and stress $\boldsymbol{\sigma}_\mu$ are known and then the micro-to-macro transition can be made by using equations (2) and (3).

On the other hand, any microscopic displacement field u_μ , may be split into the following sum:

$$\mathbf{u}_\mu(y, t) = \boldsymbol{\varepsilon}(x, t)\mathbf{y} + \tilde{\mathbf{u}}_\mu(y, t) \quad (4)$$

In equation (4) the portion $\boldsymbol{\varepsilon}(x, t)\mathbf{y}$ varies linearly in y , and it is obtained by multiplying the macroscopic strain $\boldsymbol{\varepsilon}$ imposed to the RVE, which is constant, by the coordinates of point y . The portion $\tilde{\mathbf{u}}_\mu$ is denoted displacement fluctuation and represents the strain variation in the RVE, i.e., in the case of having uniform microscopic strain $\boldsymbol{\varepsilon}_\mu$, the displacement fluctuation $\tilde{\mathbf{u}}_\mu$ is null. Accordingly, the microscopic strain field is decomposed into the following sum:

$$\boldsymbol{\varepsilon}_\mu(y, t) = \boldsymbol{\varepsilon}(x, t) + \tilde{\boldsymbol{\varepsilon}}_\mu(y, t). \quad (5)$$

where $\boldsymbol{\varepsilon}$ is constant and represents the homogeneous strain imposed to the RVE by the macro-continuum and $\tilde{\boldsymbol{\varepsilon}}_\mu$, that is denoted strain fluctuation field, can be written as $\tilde{\boldsymbol{\varepsilon}}_\mu(y, t) = \nabla^s \tilde{\mathbf{u}}_\mu$. Using the definitions in equations (1) and (5), and the linear variation of the strains fluctuation fields, it is possible to say that the macroscopic deformation $\boldsymbol{\varepsilon}$ is constant if the following condition is satisfied:

$$\int_{\partial\Omega_\mu} \tilde{\mathbf{u}}_\mu \otimes \mathbf{n} dA = 0 \quad (6)$$

Thus, writing equation (5) in the rate form, a microscopic strain rate is said to be kinematically admissible if:

$$\dot{\boldsymbol{\varepsilon}}_{\mu}(y, t) = \nabla^S \tilde{\mathbf{u}}_{\mu} = \dot{\boldsymbol{\varepsilon}}(x, t) + \dot{\boldsymbol{\varepsilon}}_{\mu}(y, t) \quad \forall \tilde{\mathbf{u}}_{\mu} \in \mathcal{T}_{\mu}^{\circ} \quad (7)$$

On the other hand, the Hill-Mandel Principle of Macro-Homogeneity, which establishes that the macroscopic stress power must equal the volume average of the microscopic stress power over the RVE, i.e., it establishes the energy consistency between the macro and micro scales. Thus, at any state of the RVE characterised by a stress field $\boldsymbol{\sigma}_{\mu}$ in equilibrium, the Principle establishes that the following identity must hold for any kinematically admissible microscopic strain rate field $\dot{\boldsymbol{\varepsilon}}_{\mu}$:

$$\boldsymbol{\sigma} : \dot{\boldsymbol{\varepsilon}} \equiv \frac{1}{V_{\mu}} \int_{\Omega_{\mu}} \boldsymbol{\sigma}_{\mu} : \dot{\boldsymbol{\varepsilon}}_{\mu} dV, \quad (8)$$

Replacing equations (7) into (8), after some manipulations we can conclude that expression (8) holds if and only if each of the following integrals vanishes individually (see more details in [1]):

$$\int_{\partial\Omega_{\mu}} \mathbf{t}^S \cdot \tilde{\mathbf{u}}_{\mu} dA = 0 \quad \forall \tilde{\mathbf{u}}_{\mu} \in \mathcal{T}_{\mu}^{\circ} \quad (9)$$

$$\int_{\Omega_{\mu}^S} b \cdot \tilde{\mathbf{u}}_{\mu} dV = 0 \quad \forall \tilde{\mathbf{u}}_{\mu} \in \mathcal{T}_{\mu}^{\circ} \quad (10)$$

Further, it is assumed that at any time t the stress at each point y of the RVE is delivered by a generic constitutive functional f_y of the strain history $\boldsymbol{\varepsilon}_{\mu}^t(y)$ at that point up to time t . This constitutive assumption, together with the equations (9) and (10) and considering $\dot{\tilde{\mathbf{u}}}_{\mu} = \boldsymbol{\eta}$ leads to the definition of the RVE equilibrium problem which consists in finding, for a given macroscopic strain $\boldsymbol{\varepsilon}$, a displacement fluctuation field $\tilde{\mathbf{u}}_{\mu} \in V_{\mu}$ such that, for each instant t , the equilibrium equation below is satisfied:

$$\int_{\Omega_{\mu}^S} \mathbf{f}_y(\boldsymbol{\varepsilon}(x, t) + \nabla^S \tilde{\mathbf{u}}_{\mu}(y, t)) : \nabla^S \boldsymbol{\eta} dV = 0 \quad \forall \boldsymbol{\eta} \in \mathcal{T}_{\mu}^{\circ} \quad (11)$$

In conclusion, for a given macroscopic strain history, we must firstly solve the RVE equilibrium problem defined by (11). With the solution $\tilde{\mathbf{u}}_{\mu}$ at hand, the macroscopic stress tensor is determined according to the averaging relation (2).

Finally, the formulation is completed with the choice of an appropriate space V_{μ} , i.e., with the choice of kinematical constraints to be imposed on the RVE. In general, different choices lead to different macroscopic response functional, [5]. In this work, the periodic boundary fluctuations will be considered in the analysis addressed in Section 4.

The periodic boundary fluctuations are typically associated with the description of media with periodic microstructure, [6]. Therefore, considering the description on two-dimensional problems, each pair i of sides of the RVE consists of equally sized subsets Γ_i^+ and Γ_i^- of $\partial\Omega_{\mu}$, with respective unit normals \mathbf{n}_i^+ and \mathbf{n}_i^- , such that $\mathbf{n}_i^- = -\mathbf{n}_i^+$.

The kinematical constraint for this class of models is that the displacement fluctuation must be periodic on the boundary of the RVE. That is, for each pair $\{y^+, y^-\}$ of boundary material points we have

$$\tilde{\mathbf{u}}_\mu(y^+, t) = \tilde{\mathbf{u}}_\mu(y^-, t) \quad \forall \{y^+, y^-\} \in \partial\Omega_\mu \quad (12)$$

3 COHESIVE FRACTURE MODEL

Composite ductile materials, with inclusions or porous, are considered to be an elasto-plastic media throughout the loading process, but on the ultimate loading regimes, these materials can present opening fractures governing the decohesion in the inclusion/matrix interface leading to a stiffness loss of the material and collapse. Therefore, in order to model the decohesion in the matrix/inclusion interface and fracture processes in the matrix, a modified cohesive fracture model is considered in this work. The cohesive fracture model has been originally proposed to simulate opening cracks in thin shells, [7]. A modified version of this model has been implemented in the finite element code on basis of multi-scale approach described in Section 2 to model the mechanical behavior of RVEs. This modified model is used in order to simulate the opening crack processes observed in ultimate loading processes in RVE of ductile porous media, mainly in the matrix/inclusion interface.

For the formulation of mixed-mode cohesive laws, there is an introduction of an effective opening displacement:

$$\delta = \sqrt{\beta^2 \delta_s^2 + \delta_n^2} \quad (13)$$

where δ_s and δ_n are the sliding and normal opening displacements, respectively. The parameter β assigns different weights to the sliding and normal opening displacements. Assuming that free energy potential ϕ depends on δ , the cohesive law is written as:

$$\mathbf{t} = \frac{t}{\delta} (\beta^2 \boldsymbol{\delta}_s + \delta_n \mathbf{n}) \quad (14)$$

The \mathbf{n} vector is normal to the crack, $\boldsymbol{\delta}_s$ is the sliding opening displacement vector located on the crack surface, \mathbf{t} is the cohesive traction vector over the crack and t is a scalar effective traction.

In this work we have modified the cohesive law proposed by [7] in order to simulate a fracture behavior in ductile media. The relations proposed are described in the following equations:

$$t = \sigma_c e^{-\delta/\delta_c} \quad \text{if } \delta = \delta_{max} \text{ and } \dot{\delta} \geq 0 \quad (15)$$

$$t = \frac{t_{max}}{\delta_{max}} \delta \quad \text{if } \delta < \delta_{max} \text{ or } \dot{\delta} < 0 \quad (16)$$

where e is the e-number, σ_c is the maximum cohesive normal traction and δ_c is a critical opening displacement. Also, in this work, the cohesive law presents an elastic unloading (equation (16)), but this limitation is not important for this work because we are dealing with increasing loading. Observe that we have tried to attend the methodology proposed by [7], where there is no fracture in the material a priori. But, when the effective traction on the possible fracture assumes value bigger than σ_c , the fracture is then created considering a gradual separation process in order to avoid the strong discontinuity in the material. Also, the critical opening displacement is approximately given by $\delta_c = 2G_c/\sigma_c$, where G_c is the mode

I fracture energy density.

The conformity of the triangle finite elements before the nucleation of fractures is imposed by the addition of a penalty factor (λ_p), i. e., the cohesive contact finite elements are introduced on the boundaries of the triangle finite elements before the nucleation of the fractures. This strategy is called intrinsic cohesive elements [8] and it is easier to develop a mesh generation code because all cohesive contact elements are embedded in the discretized structure prior to the beginning of simulation.

This penalty factor is a scalar value parameter. In practice use, high values for the penalty factor are adopted in order to obtain a sufficiently accurate approximation.

In general way, this strategy intends to create stiffness in the node-pairs at the cohesive contact finite element in order to not allow the penetration of the crack surfaces. On the other hand, in tension regimes, this penalty factor effectively amounts to replacing the initial rigid portion of the cohesive law by a stiff linear response of the form [7]:

$$t = \lambda_p \delta \quad \text{if } \lambda_p \delta \leq \sigma_c \quad (17)$$

For detection of the contact phenomenon, this work adopts the concept of the gap between the Gauss points of the cohesive contact finite element. In this work, the cohesive contact finite element are inserted between triangular finite elements. These kinds of models and finite elements supply accurate responses despite their simplicity, avoiding the need of an adaptive insertion of cohesive elements. Our goal is to model the mechanical behavior of composite materials that present plasticity and fracture processes using mathematical models as simplest as possible by means of a computational homogenization-based approach.

The class of elements considered in this work is composed by two surface elements which coincide to the undeformed reference configuration of the RVE as shown in Figure 2. The cohesive contact element is defined with 4 (four) nodes being its geometry compatible with the two-dimensional triangular elements used to model the matrix and inclusion phases.

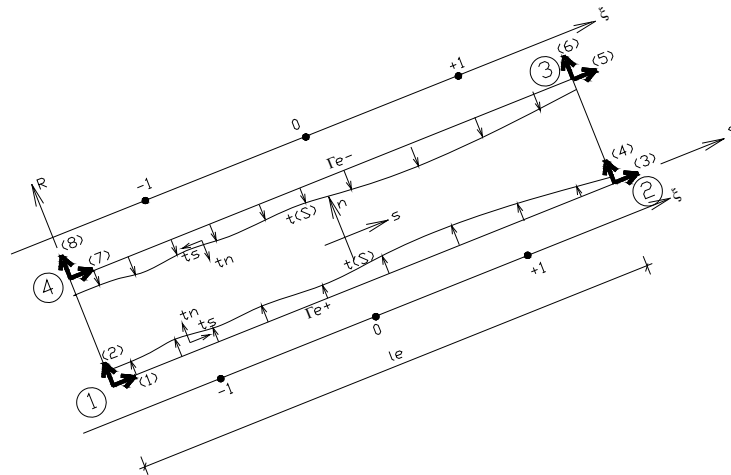


Figure 2 Geometry of cohesive contact finite element

First, consider the local system of the finite element given by s (sliding direction) and n

(normal direction) coordinate axes (see Figure 2). The nodal displacements and internal forces vectors are given by:

$$\mathbf{u}_e = \begin{Bmatrix} u_e(1) \\ \vdots \\ u_e(4) \\ u_e(5) \\ \vdots \\ u_e(8) \end{Bmatrix} = \begin{Bmatrix} \mathbf{u}_e^+ \\ \mathbf{u}_e^- \end{Bmatrix} \quad \text{and} \quad \mathbf{F}_e^{\text{int}} = \begin{Bmatrix} F_e^{\text{int}}(1) \\ \vdots \\ F_e^{\text{int}}(4) \\ F_e^{\text{int}}(5) \\ \vdots \\ F_e^{\text{int}}(8) \end{Bmatrix} = \begin{Bmatrix} \mathbf{F}_e^{\text{int}+} \\ \mathbf{F}_e^{\text{int}-} \end{Bmatrix} \quad (18)$$

The \mathbf{u}_e^+ and $\mathbf{F}_e^{\text{int}+}$ are the nodal displacements and internal forces vectors related to plus side Γ_e^+ . Similarly, the \mathbf{u}_e^- and $\mathbf{F}_e^{\text{int}-}$ are the nodal displacements and internal forces vectors related to minus side Γ_e^- .

In order to compute the Gap Function in each Gauss point, the following expression is used:

$$\delta_e(\xi_i) = \mathbf{N}_e^-(\xi_i(s))\mathbf{u}_e^- - \mathbf{N}_e^+(\xi_i(s))\mathbf{u}_e^+ = u^-(\xi_i) - u^+(\xi_i), i = 1,2,3 \text{ Gauss point} \quad (19)$$

where $u^-(\xi_i)$ and $u^+(\xi_i)$ are the displacements related to Gauss point on minus and plus surface, respectively. $\mathbf{N}_e^-(\xi_i(s))$ and $\mathbf{N}_e^+(\xi_i(s))$ are shape functions related to Gauss point on minus and plus surfaces, respectively.

After some trite calculations, it is possible to obtain the internal force vector at the cohesive contact finite element as follows:

$$\mathbf{F}_e^{\text{int}+} = \frac{l_e}{2} \int_{-1}^{+1} \mathbf{N}_e^{\text{T}}(\xi) \mathbf{t}(S(\xi)) d\xi \quad (20)$$

where l_e is the finite element length and $\mathbf{t}(S(\xi))$ is the cohesive traction vector on each Gauss point composed by sliding and normal components. It is important to note that each Gauss point contributes to the internal force evaluation by means of the traction vector computed either by the cohesive law (if a crack is opened at that Gauss point) or by the contact law (if a crack is closed at that Gauss point). Therefore, the crack surfaces obtained can be not properly parallel.

On the other hand, the RVE discrete non-linear boundary value problem is solved by the linearization of the following equilibrium equation:

$$\mathbf{R} + \frac{d\mathbf{F}}{d\mathbf{u}} d\tilde{\mathbf{u}} = 0 \quad (21)$$

where \mathbf{R} is the out-of-balance force and $d\tilde{\mathbf{u}}$ is the increment of displacement fluctuation field and calling \mathbf{K} the tangent stiffness as $\mathbf{K} = \frac{d\mathbf{F}}{d\mathbf{u}}$. Then, focusing on the cohesive contact finite element, the consistent tangent stiffness \mathbf{K}_e is written as:

$$\mathbf{K}_e = \frac{d\mathbf{F}_e^{\text{int}}}{d\mathbf{u}_e} = \begin{bmatrix} \frac{d\mathbf{F}_e^{\text{int}+}}{d\mathbf{u}_e} \\ \frac{d\mathbf{F}_e^{\text{int}-}}{d\mathbf{u}_e} \end{bmatrix} \quad (22)$$

Note that in eq (22) the component related to minus side must take into account the direction of cohesive traction vector at that surface.

4 NUMERICAL RESULTS

All simulations carried out in this section have been performed by employing the computational homogenization under the plane stress assumption in small strain regime. Besides, the RVEs are squares, being their dimensions defined by $L \times L$ and their thickness given by $L/10$. The average stress is obtained by imposing the macro-strain over the RVE and subsequently solving the microscopic initial boundary value problem for the defined boundary condition assumed. It has been used 10^{-6} as tolerance factor in order to check the convergence of the non-linear procedure.

The material properties assigned for the matrix are: Young's modulus $E = 200$ GPa, Poisson's ratio $\nu = 0.3$, initial yield stress $\sigma_y = 200$ MPa and strain hardening modulus $H = 30$ GPa. To simulate the elastic behavior of the inclusion $E = 21$ GPa and $\nu = 0.2$ have been adopted. Finally, the material parameters of the interface zone have been assumed as: $\delta_c = 2 \times 10^{-5}$ m, $\sigma_c = 0.1$ MPa, $\beta = 0.707$ and $\lambda_p = 3 \times 10^6$.

Here and after, it is understood that on the initial loading stage, the materials present an elastoplastic behavior whereas on the rupture stages the material presents a fracture process in the matrix and ITZ as well as an elastoplastic behavior. As boundary conditions, periodic and linear conditions have been considered. The applied load is given by a macro-strain tensor $\epsilon = [-0.00099; 0.0033; 0]$ divided in 10 increments, which represents an uniaxial tension in y direction (see Fig. 01). Initially, Fig. 3 shows the numerical results of a RVE that contains a ductile material. For the initial loading stage configuration 8 triangle finite elements have been used whereas for the rupture stage configuration, 684 triangle finite elements and 26 cohesive contact finite elements have been considered. Note that the fracture process leads to a substantial decreasing of both the strength and material stiffness which reflects the complete failure of the microstructure. Besides, both the periodic and linear boundary conditions present the same numerical response for the plastic behavior adopted in this example. However, on the rupture stage the periodic condition presents a more flexible response when the fracture process takes place in the matrix zone. Once more, the increasing of the number of required iterations to solve the equilibrium problem is observed during the rupture loading stage although the proposed modeling has presented a quadratic rate of asymptotic convergence of the Newton–Raphson scheme.

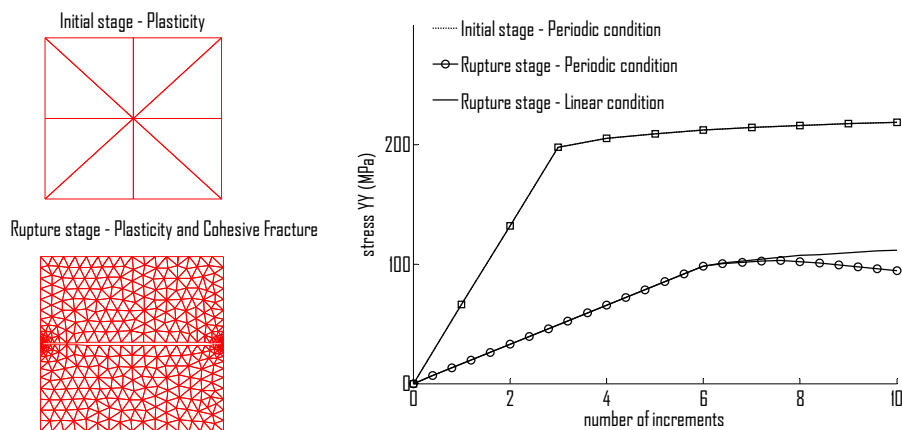


Figure 3 Progressive failure of the ductile material microstructure.

Now, a porous ductile material depicted in Fig. 4 is modeled. For the initial loading stage and the rupture stage have been adopted, respectively, 508 and 676 triangle finite elements. Besides, 22 cohesive contact finite elements have been considered for the rupture stage. The same behavior of the ductile material is observed in this case although the strength and RVE rigidity are smaller than the ones related to the ductile material due to the presence of the porosity.

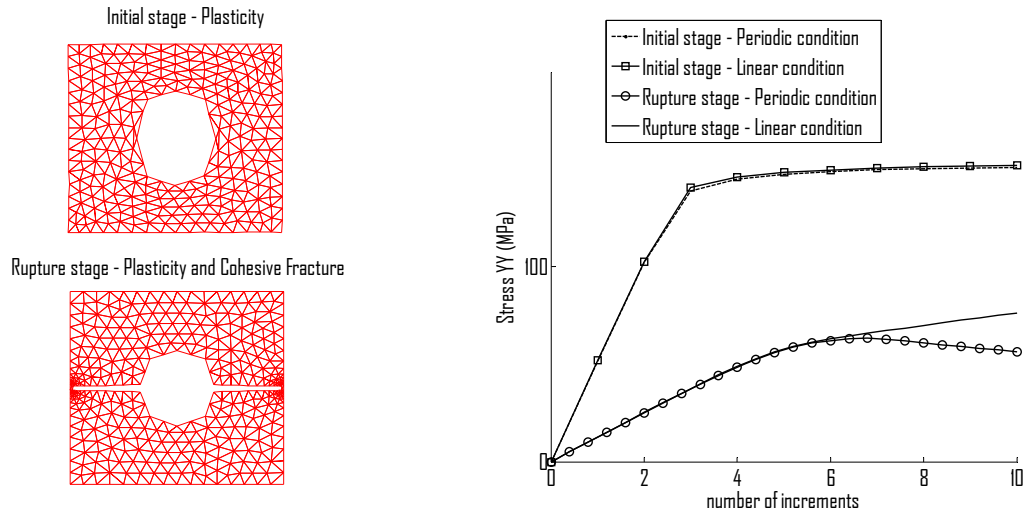


Figure 4 Progressive failure of the porous ductile microstructure ($v_f = 10\%$).

The last analysis deals with metal matrix composite microstructure. For the initial loading stage configuration 511 triangle finite elements have been adopted to model the matrix whereas 73 triangle finite elements have been used to model the inclusion. For the rupture stage configuration, 16 cohesive contact finite elements have been also considered to model the ITZ (see Fig. 5). In this case only periodic boundary conditions have been assumed in the RVE. Note that the decohesion process becomes more evident in the mechanical behavior of the RVE when the opening fracture occurs at a intermediate stage. This process leads to a softening regime despite of having a plastic matrix and an elastic inclusion. Besides, the contact problems arise in the ITZ leading to the increasing of the number of required iterations. Soon after, when the RVE presents fractures on the matrix zone (rupture regime), a substantial decreasing of the material's strength evidences the complete failure of the microstructure.

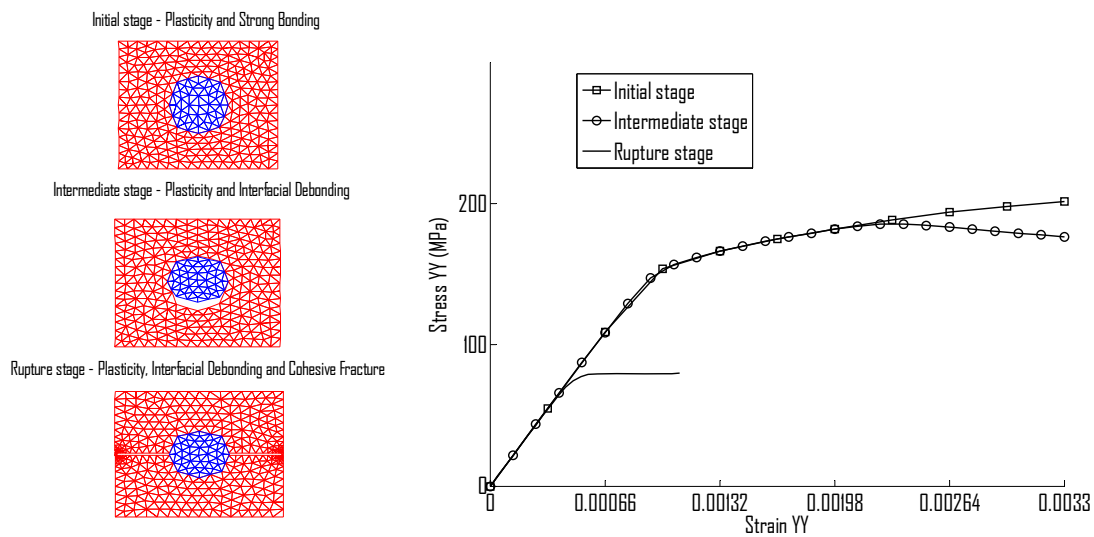


Figure 5 Progressive failure of the metal matrix ductile microstructure ($v_f = 10\%$).

5 CONCLUSIONS

In this work, numerical applications of a computational homogenization-based approach proposed to model the mechanical behavior of heterogeneous materials have been presented. A cohesive contact finite element as well as a cohesive law have been described. This proposed modeling has been implemented in a 2D finite element code to analyze RVEs within a purely kinematical multi-scale framework developed by [1,5].

The qualitative responses are quite satisfactory evidencing the good description of the micromechanical behavior of the RVEs composed by ductile metal matrix considering porous or elastic inclusions. Besides, the debonding phase in this kind of material has been considered. The results show that the modeling developed in this work is potentially applicable in multi-scale analysis of composite structures in initial and rupture loading stages.

ACKNOWLEDGEMENTS

The financial supports from CAPES Foundation, Ministry of Education of Brazil (Grant n. BEX 0805/11-4), CNPq (National Council for Scientific and Technological Development) and FAPEG (Goiás Research Foundation) are gratefully acknowledged.

REFERENCES

- [1] Peric, D., de Souza Neto, E. A., Feijóo, R. A., Partovi, M. and Carneiro Molina, A. J.. On micro-to-macro transitions for multiscale analysis of heterogeneous materials: unified variational basis and finite element Implementation. *Int J Numer Meth Eng* (2010) **87**: 149-170.
- [2] Azizi R. Micromechanical modeling of damage in periodic composites using strain gradient plasticity. *Eng Fract Mech* (2012) **92**: 101-113.
- [3] De Souza Neto, E. A. , Peric, D. and Owen, D. R. J.. *Computational Methods for Plasticity: Theory and Applications*. 1st ed. West Sussex:Wiley, (2008).
- [4] Pituba, J. J. C. and de Souza Neto EA. Characterization of macroscopic mechanical

- behavior of concrete with mesoscopic scale finite element analysis. *European Congress on Computational Methods in Applied Sciences and Engineering (ECCOMAS 2012)*. J. Eberhardsteiner et.al. (eds.), Vienna, Austria, (2012).
- [5] Giusti, S. M., Blanco, P. J., de Souza Neto, E. A. and Feijóo, R. A.. An assessment of the Gurson yield criterion by a computational multi-scale approach. *Eng Computation* (2009) **26**: 281-301.
- [6] Somer, D. D., de Souza Neto, E. A., Dettmer, W. G. and Peric, D.. A sub-stepping scheme for multi-scale analysis of solids. *Comput Method Appl M* (2009) **198**: 1006-1016.
- [7] Cirak, F., Ortiz, M. and Pandolfi, A.. A cohesive approach to thin-shell fracture and fragmentation. *Comput Method Appl M* (2005) **194**: 2604-2618.
- [8] Paulino, G. H., Celes, W., Espinha, R. and Zhang, Z.. A general topology-based framework for adaptative insertion of cohesive elements in finite element meshes. *Eng Comput* (2008) **24**: 59-78.